Geomechanics and Engineering, *Vol. 26, No. 2 (2021) 133-146*
https://doi.org/10.12989/gae.2021.26.2.133

Explicit finite element analysis of slope stability by strength reduction

Morteza Naeij[1], Hussein Ghasemi[2], Danial Ghafarian[1] and Yousef Javanmardi*[3]

[1]*Department of Civil and Environmental Engineering, Amirkabir University of Technology (Tehran Polytechnic), Hafez Ave., Tehran, Iran*
[2]*School of Civil Engineering, College of Engineering, University of Tehran, Tehran, Iran*
[3]*Department of Mechanical Engineering, University College London, London, U.K.*

(Received April 30, 2020, Revised February 11, 2021, Accepted June 27, 2021)

Abstract. The construction of stable slopes and vertical cuts is an important step in many geotechnical projects. Limit equilibrium methods (LEMs) are well-accepted procedures to compute factors of safety (FoS); however, they fail to provide any information about the distribution of the field variables within the soil mass because they do not include any stress-strain relationship in their formulation. On the other hand, the iterative finite element method (FEM/I) can estimate the field variables, but in the current study, we show that, for steep slopes and vertical cuts, it underestimates the FoS compared to the LEM. To overcome the obstacles that exist in this method, this study proposes a new approach to define the initiation of instability based on an abrupt change in the kinetic energy of the system. We also suggest a procedure to calculate the minimum FoS based on the explicit finite element method (FEM/E). Comparison of the results obtained from the proposed method, LEM, and FEM/I revealed that the FoS computed by the proposed method is in good agreement with the results of the LEM for a wide range of material parameters, geometries and external loading conditions, while no assumption regarding the critical slip surface needs to be made.

Keywords: explicit finite element method (FEM/E); factor of safety (FoS); kinetic energy; strength reduction method (SRM)

1. Introduction

Analysing slope stability and determining the factor of safety (FoS) are some of the most prevalent geotechnical problems. The limit equilibrium method (LEM), a conventional and well-established method for assessing the FoS of slopes and geotechnical structures, is routinely used by geotechnical engineers and researchers. Although the LEM is well accepted by many engineers to calculate the FoS for common geotechnical practices, this method does not consider the stress-strain relationship and progressive failure of the soil (Morgenstern and Price 1965). In other words, it is assumed in this method that no deformation occurs in the soil mass before the failure conditions, and as soon as the failure conditions on the slip surface are met, the deformations on this surface will be unlimited. Under failure conditions, the shear strength on the slip surface is fully generated. Due to the indeterminate nature of the problem, assumptions have to be made for estimating the distribution of stresses on the slip surfaces and in the soil mass. Furthermore, the geometry of the slip surface needs to be assumed in the LEM.

Increasing calculation speed of desktop computers and progress in their computational capabilities provided opportunities for researchers to calculate the FoS based on distributed stresses in the soil domain with the aid of the finite element method (FEM). Zienkiewicz *et al.* (1975) proposed a strength-reduction procedure for the FEM to calculate the FoS of soil structures, in which the strength parameters of the soil are reduced gradually until the slope fails. Then, the FoS is computed by dividing the initial strength parameters by the reduced parameters (Tu *et al.* 2016a, b, Kaveh *et al.* 2018). This methodology has been extended for various geotechnical problems, such as embankments, slopes, and mines (Griffiths and Lane 1999, Cheng *et al.* 2007, Abusharar and Han 2011, Li *et al.* 2012, Dyson and Tolooiyan 2018). Despite the LEM, applying the stress-strain relationship in the FEM determines the critical slip surface based on elastoplastic constitutive models, and progressive failure is captured (Zhao *et al.* 2017). Considering the stress distribution in the soil domain provides an opportunity for researchers to include the variation in field data in their slope analyses (Liu *et al.* 2017, Dyson *et al.* 2019). Additionally, the FoS in non-heterogeneous soil can be calculated (Xu *et al.* 2006, Zhu *et al.* 2015).

Researchers have suggested various criteria for calculating the minimum FoS of slopes and proposed different ways to define the critical slip surface based on the strength-reduction method (SRM) using the iterative finite element method (FEM/I). Matsui *et al.* (1992) suggested that the slip surface should extend from the toe of the slope to its top surface and that plastic strain should govern through this surface. Many researchers (Zienkiewicz *et al.* 1975, Griffiths and Lane 1999, Cheng *et al.* 2007, Griffiths and Marquez 2007) applied iterative finite elements and suggested that due to a reduction in soil strength parameters, when the instability starts in the slope, the

*Corresponding author, Ph.D.
E-mail: y.javanmardi@ucl.ut.uk

ISSN: 2005-307X (Print), 2092-6219 (Online)

numerical model fails to converge. Therefore, the magnitude of the reduction factor at the beginning of divergence is considered as the FoS. In addition, sometimes the FoS, using the FEM/I, is calculated based on predefined iteration numbers. On the other hand, Crisfield (1997) argued that non-convergence does not necessarily mean the collapse of structures and Nie *et al.* (2019) proposed a new method which relies on the convergence in solution and Wei *et al.* (2020) applied a procedure to calculate FoS based on slope geometry. Dawson *et al.* (1999) and Dawson *et al.* (2000) proposed a procedure based on strength reduction for the finite difference method (FDM) to calculate the FoS in slope stability analysis and implemented their method in the FLAC program (Itasca 2000). They suggested that the FoS can be calculated by monitoring the trend of out-of-balance force in the nodes of the finite difference model. The out-of-balance force increases significantly due to instability in the model, which could be a sign of failure in the soil mass.

In contrast to the available FEM/I approach, which performs many iterations to simulate the unstable condition, a new criterion based on kinetic energy is employed in the current study to define the failure condition. Furthermore, despite the FEM/I, we adopt an incremental approach based on an explicit finite element method (FEM/E). To compute the minimum FoS for soil slopes, ABAQUS/Explicit (Systèmes 2014) is used, and an implemented Mohr-Coulomb constitutive model (VUMAT), in addition to a PYTHON script, is developed (https://doi.org/10.5281/zenodo.4498843). The ability of the new strategy is evaluated by modelling different geometries and various external loading conditions, i.e., a surcharge and pseudo-static earthquake load, using a wide range of strength properties for the soil. Then, the results are compared with the existing methods (LEM and FEM/I). This demonstrates that the FoS computed using the proposed procedure is consistent with that calculated using the LEM in all cases, whereas no assumption about the slip surface needs to be made, while the field variables, such as displacement or strain, are computed in the soil domain at the same time. This comparison also shows that for vertical cuts, the computed FoS using the FEM/I is not in great agreement with the results obtained from the LEM, which is an accepted method by researchers and engineers to calculate the FoS, while the new procedure proposed in the current study does not suffer from such a deficiency.

2. Numerical procedure

For many years, a strength-reduction strategy in the FEM/I was applied to calculate the minimum FoS of geotechnical structures. In this method, the strength parameters (cohesion and friction angle) are reduced by dividing their initial value by strength reduction factor (SRF). Due to excessive deformation, convergence could not be achieved after many iterations and the SRF relates to the minimum FoS in the soil mass. On the other hand, FEM/E has proven its eligibility for simulations with possible severe distortion or models with extremely deformable materials. Therefore, it is almost impossible to apply non-convergence methodologies in the FEM/E for calculating the minimum FoS of slopes and another criterion needs to be applied. To comprehend the proposed method, a brief explanation of the FEM/E and its modelling procedure is presented in the following section.

2.1 Finite element analysis

The finite element explicit procedure executes the numerical modelling through a large number of small-time increments. In ABAQUS/ Explicit, an explicit central-difference time integration rule is used. The explicit dynamics analysis procedure is based on the implementation of an explicit integration rule together with the use of lumped mass to reduce the cost of simulation (Systèmes 2014):

$$\dot{u}^N_{(i+\frac{1}{2})} = \dot{u}^N_{(i-\frac{1}{2})} + \frac{\Delta t_{(i+1)} + \Delta t_{(i)}}{2}\ddot{u}^N_{(i)}$$
$$u^N_{(i+1)} = u^N_{(i)} + \Delta t_{(i+1)}\dot{u}^N_{(i+\frac{1}{2})} \quad (1)$$

where Δt is a critical time increment, u^N is a degree of freedom and the subscript *i* refers to the increment number in an explicit dynamic step (N). The central-difference integration operator is explicit in the sense that the kinematic state is advanced using known values of $\dot{u}^N_{(i-\frac{1}{2})}$ and $\ddot{u}^N_{(i)}$ from the previous increment. The explicit procedure requires no iterations. The internal force vector is assembled from contributions of the individual elements such that a global stiffness matrix does not need to be formed (Systèmes 2014). The central-difference operator is conditionally stable (Bathe 2006), and the stability limit for the operator with no damping is given in terms of the highest frequency of the system as follows:

$$\Delta t \leq \frac{2}{\omega_{max}} \quad (2)$$

where ω_{max} is the highest frequency of the system. An approximation to the stability limit is often written as the smallest transit time of a dilatational wave across any of the elements in the mesh domain. Therefore, the stable time increment relates to the material elastic parameters and mesh dimension. To obtain results close to the static condition, the ratio of the total kinetic energy to the total internal energy of an executed model should be kept less than 5% throughout most of the simulation (Systèmes 2014).

Finite element explicit method has proven its eligibility for simulations with possible severe distortion or models with extremely deformable materials. Therefore, it is almost impossible to apply non-convergence methodologies in the FEM/E for calculating the FoS of slopes and another criterion needs to be applied.

2.2 Constitutive model

In the FEM/E, as a finite element procedure, the stress-strain relationship is used to calculate the stress and strain in the model. Using an elastic-perfectly plastic constitutive model provides the advantage of quick transition from the

elastic condition to fully plastic behaviour in the soil (Dawson *et al.* 1999). Therefore, the reduction in the soil strength parameters initiates the failure condition in the weakest surface, where the mobilised shear stress surpasses the shear resistance. In this study, we employed the Mohr-Coulomb model using the code developed by Naeij *et al.* (2019) and Naeij and Soroush (2021) in favour of access to constitutive model parameters (https://doi.org/10.5281/zenodo.4498843). The code was implemented into ABAQUS/Explicit as a VUMAT sub-routine. Here, we used the associated flow rule without considering softening/hardening.

2.3 Strength-reduction procedure

The FoS in the strength-reduction method is defined as follows:

$$C_{failure} = \frac{C_{ini}}{SRF}$$
$$\varphi_{failure} = tan^{-1}(\frac{\tan(\varphi_{ini})}{SRF}) \quad (3)$$
$$\text{FoS}=\text{SRF}_{\text{at failure}}$$

where φ_{ini} and C_{ini} are the initial values of the friction angle and cohesion, respectively, and $\varphi_{failure}$ and $C_{failure}$ are the friction angle and cohesion, respectively, that cause imminent failure. To obtain the minimum value of the FoS, the FEM needs to change the SRF factor gradually (decrease SRF when FoS>1 and increase SRF if FoS<1).

2.4 Calculation of the FoS

ABAQUS could not calculate the FoS automatically, and it does not have a built-in section to change the material parameters and apply the SRF. Therefore, a code based on PYTHON was written to change the Mohr-Coulomb strength parameters (see supplementary data). After each change in strength parameters, the model with the new parameters executes automatically with the aid of the PYTHON code. At the end of each execution, the maximum kinetic energy during gravitational loading is obtained from the output database file and compared with the kinetic energy after loading. Due to the dynamic nature of the explicit finite element, applying an external load to the model abruptly may cause shock wave generation. To conduct quasi-static analysis, it is necessary to apply gravitational load to the model smoothly and in a few seconds. Fig. 1.a shows the loading procedure. According to this figure, gravitational acceleration is applied smoothly in 5 seconds (simulation time), and this load remains constant from 5 to 5.5 seconds.

The basis of the proposed procedure in this study is monitoring kinetic energy (Eq. (4)) in the time of applying gravity (0 to 5 seconds) and checking the magnitude of kinetic energy slightly after this time with no change in loading conditions. If a part of the model (a block of soil on the slip surface corresponding to the minimum FoS) experiences instability, the term of kinetic energy shows a drastic increase at the end of the simulation (Fig. 1(e)). In Fig. 1(e), a sharp increase in the magnitude of kinetic energy after loading indicates that there is significant movement in a block of the model. The reduced (or increased) soil strength parameters that led to the initiation of instability are used to calculate the FoS. The SRFs for the stable and failure conditions in Fig. 1(f) are 1.16 and 1.17, respectively (for a 1 H-1 V slope with c=4 kPa, φ=39º, γ=19 kN/m^3, E=20 kPa and ν=0.2). The magnitude of kinetic energy during gravitational loading (0-5 seconds) is the same, but at the end of gravity loading, the trend of kinetic energy shows different directions for stable and failure conditions. This means that with a small change in the SRF of two successive executions, the trend of kinetic energy shows a dramatic difference for the failure condition.

$$E_{KE} = \frac{1}{2}\int_V \rho \dot{U}^T \dot{U} dV \quad (4)$$

Although the whole model shows a stable condition, the kinetic energy of the model increases only due to movement of a block of soil. This block slides on a surface, which is known as the critical slip surface. For stable conditions, due to the stability of the soil mass, the kinetic energy decreases slightly compared to its maximum value during loading. In other words, the decrease in the magnitude of kinetic energy at the end of the loading period means that the strength parameters are sufficient to keep the whole model stable, and further reduction in their value is required to initiate the instability.

If the kinetic energy shows smaller magnitudes at the end of execution compared to its maximum value during the gravity loading period, the PYTHON code changes the strength parameters in the next execution. For cases suffering from instability at the beginning (i.e., FoS<1), a large number (i.e., $\frac{1}{SRF}$ when $SRF < 1$) is applied to the strength parameters to provide stability for the model at the beginning of analysis. Then, similar to the models with initial stable conditions (FoS>1), these parameters decrease gradually. Finally, at a specific SRF, the magnitude of the kinetic energy increases suddenly, and the model will experience instability. The SRF at the beginning of failure is considered as the FoS again. Fig. 2 shows flow diagram of the proposed procedure.

All models in this study were prepared by applying nonlinear geometry (the geometrical coordinates of nodes were updated according to their computed displacement). The ratio be;tween the internal energy and the kinetic energy is less than 1% (in the stable model) to maintain the simulation under static conditions. Due to employing the associate flow rule, elastic constants, the stress path, stage construction, and initial stress have no effect on the FoS (Dawson *et al.* 2000) and were not addressed in this study.

Liu *et al.* (2018) showed that applying full integration or reduced integration elements has a negligible effect on the minimum FoS of slopes. In all models in this study, unstructured, reduced integration quadrilateral element (CPE4R) for 2D (plane strain) simulation were applied, and an average mesh size of 0.5 meter was selected and the effects of mesh size will be discussed later. Side boundaries were fixed in the X direction only, and the base of the

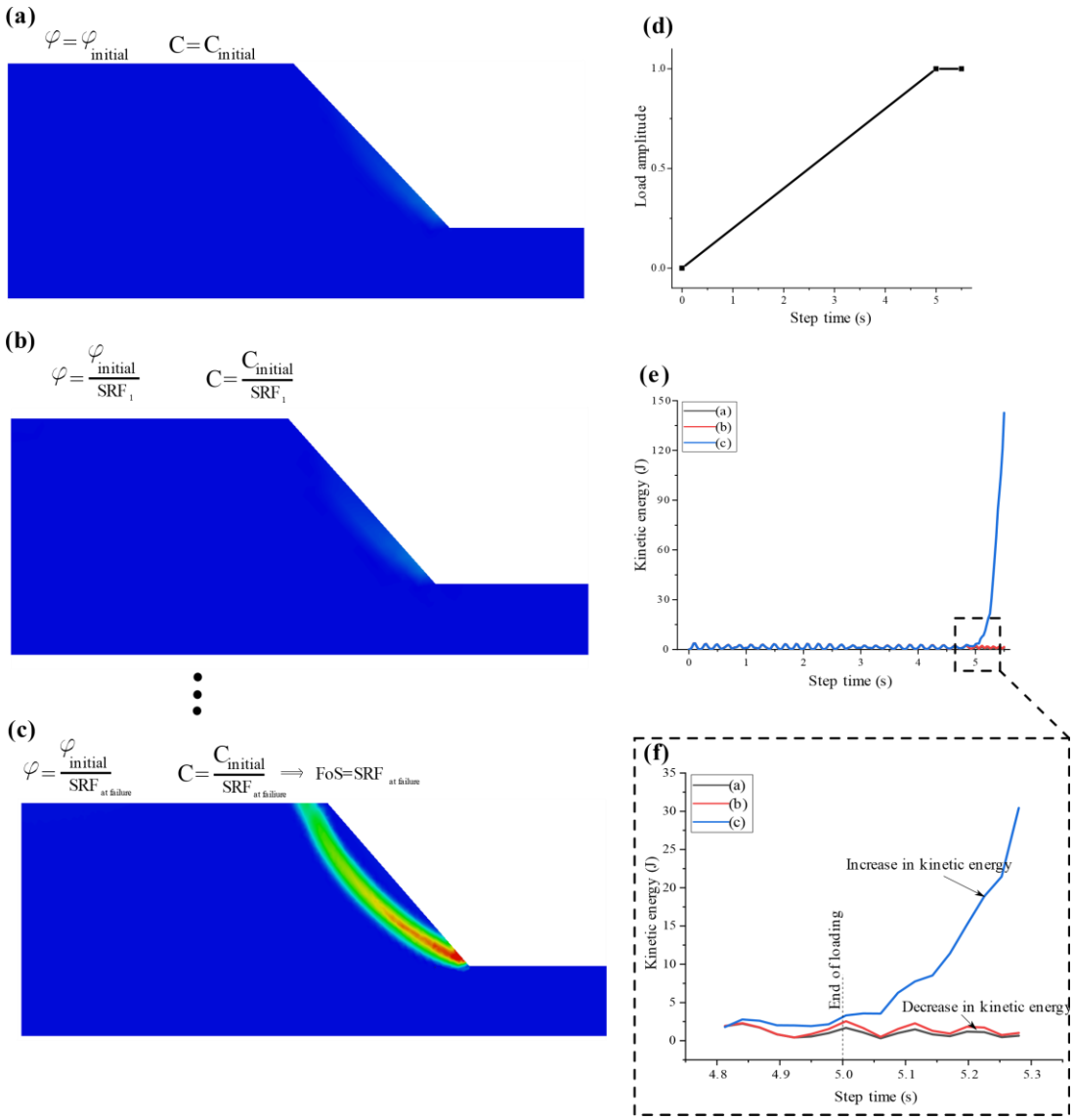

Fig. 1 Schematic representation of the strength reduction method: (a) At the first step, simulation is carried out using the original strength parameters of the soil, (b) Then, the strength parameters are reduced by dividing the initial values by the SRF, (c) This reduction continues until the failure initiates, (d) For dynamic explicit simulations, the gravitational load amplitude increases linearly within five seconds and then becomes constant (e) and (f). Kinetic energy slightly decreases for no failure conditions (a) and (b), while it increases abruptly immediately after initiation of the failure (c)

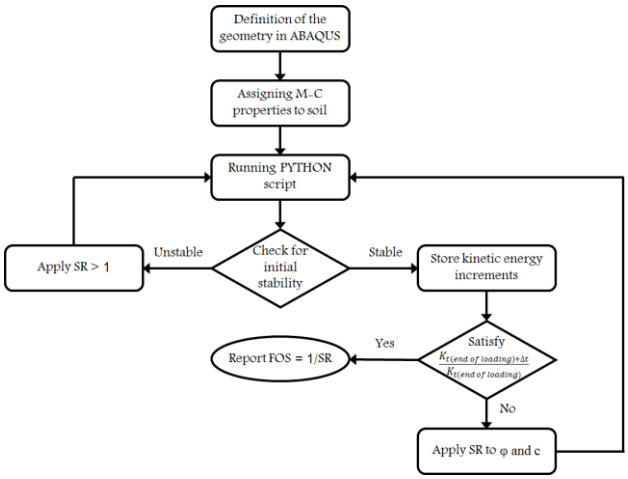

Fig. 2 Flow diagram of proposed procedure for calculating the minimum FoS of slopes in FEM/E

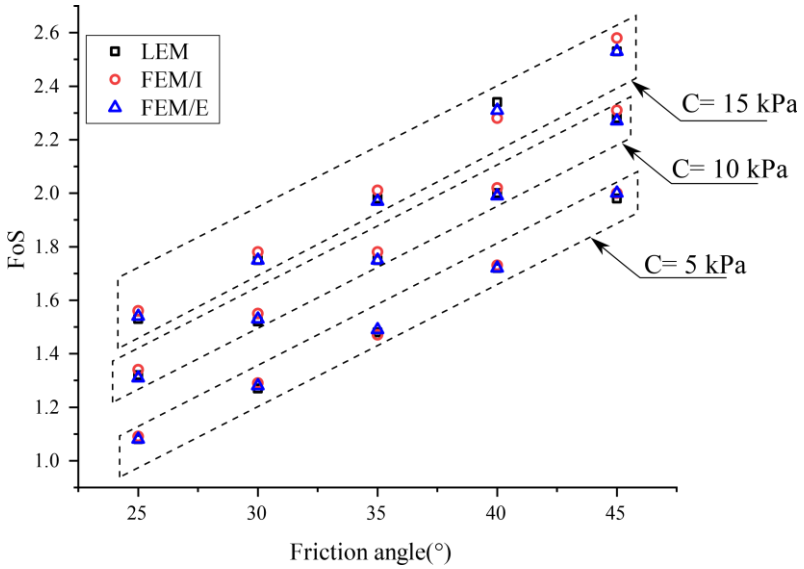

Fig. 3 Results of the FEM/E, LEM, and FEM/I for 1.5 H-1 V slope

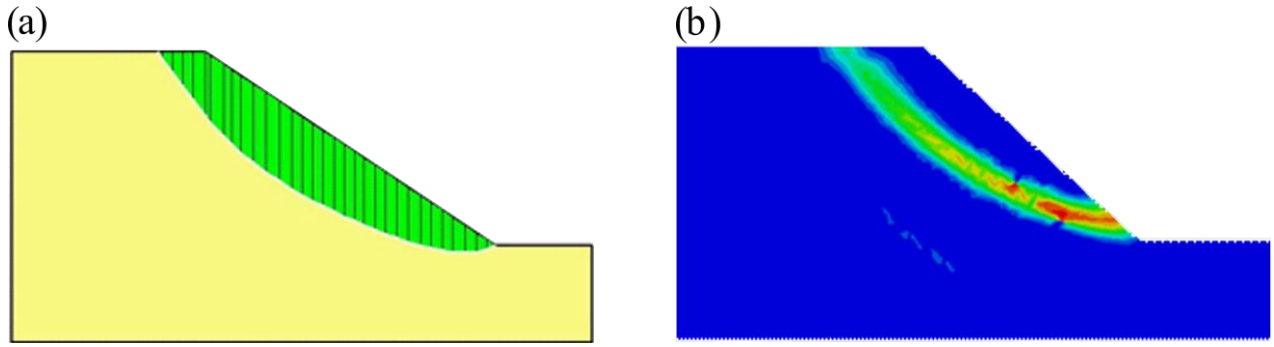

Fig. 4 Shape of the critical slip surface for soil with φ=45º, C=10 kPa (a) LEM (FoS=2.28) and (b) FEM/E (FoS=2.27)

models was fixed in both directions.

3. Results

To investigate the potential of the presented procedure for calculating the minimum FoS of soil slopes, the results of the FEM/E from ABAQUS/Explicit were compared with the results of the LEM based on the Morgenstern-Price method (Morgenstern and Price 1965) using Slope/W (Geo-slope Ltd. 2012) and FEM/I from PLAXIS (Brinkgreve *et al.* 2014).

Slopes were simulated with slope angles ranging from 33.6º (1.5 H-1 V) to 90º (i.e., excavation). The range of the soil internal friction angle was from 0º to 45º and cohesion ranged from 2 to 55 kPa. In addition, surface loads from 10 to 60 kPa and three pseudo-static horizontal seismic accelerations (0.2 g, 0.25 g, and 0.3 g) were applied and compared with two conventional methods.

3.1 Slope 1.5 H-1 V

Fig. 3 presents the calculated minimum FoS for slopes with 1.5 H-1 V based on changing the magnitude of the kinetic energy in the model and its comparison to the LEM and FEM/I. For this slope, the results show good agreement between the three methods, and the minimum FoSs of these three methods are approximately the same. Fig. 4 shows that the shear strain contour represents the critical slip surface for the FEM/E and the critical slip surface based on the LEM analysis. From this figure, there is good agreement between the shape of the slip surface and its depth in the FEM/E and LEM. Therefore, in addition to good agreement for minimum values of the FoS, the shape of critical slip surfaces in the FEM/E are similar to those in the LEM.

3.2 Slope 1 H-1 V

Fig. 5 shows the calculated minimum FoS for a slope with a gradient of 45º (1 H-1 V) with a homogenous single layer and based on the proposed method and its comparison with the LEM and FEM/I. For this slope, the results show excellent agreement between the three methods. The friction angle (φ) changed from 30º to 39º in three-degree intervals in Figs. 5(a) to 5(d), and the cohesion (C) changed over a wide range to show the ability of the proposed method to compute the minimum FoS in a wide range of soil strength parameters. The magnitude of C was changed in 1 and 5 kPa intervals for each selected φ. The minimum FoS for small and large changes in the magnitude of C shows that the proposed method could calculate the minimum FoS with enough accuracy even with small

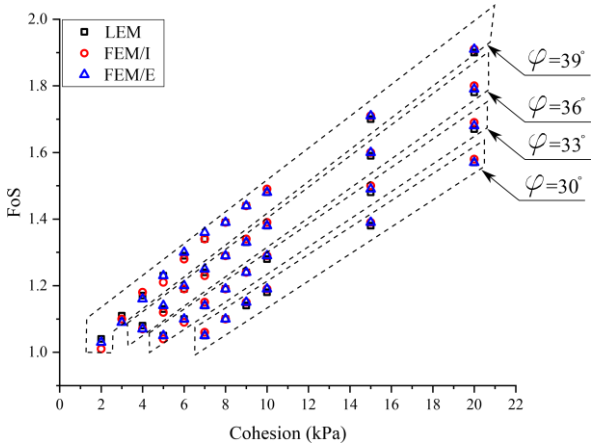

Fig. 5 Results of the LEM, FEM/I and FEM/E for 1 H-1 V slope

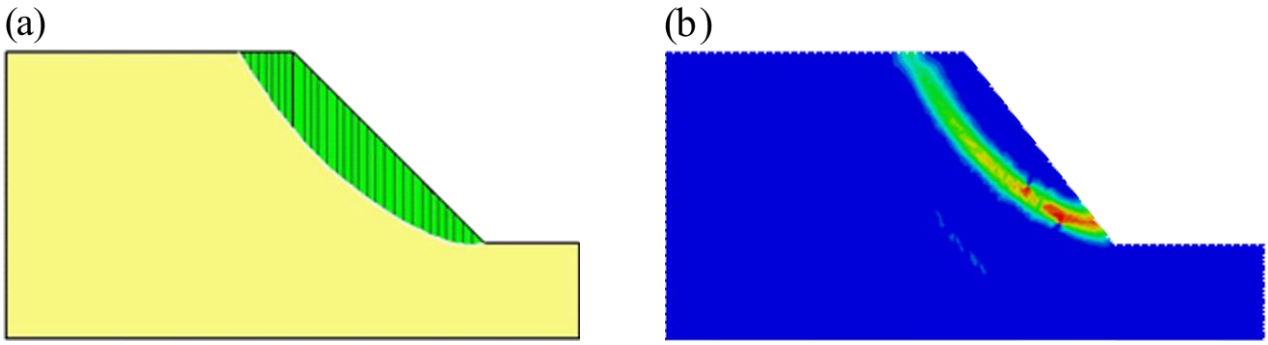

Fig. 6 Shape of the critical slip surface for soil with φ=39º, C=20 kPa (a) LEM (FoS=1.90) and (b) FEM/E (FoS=1.91)

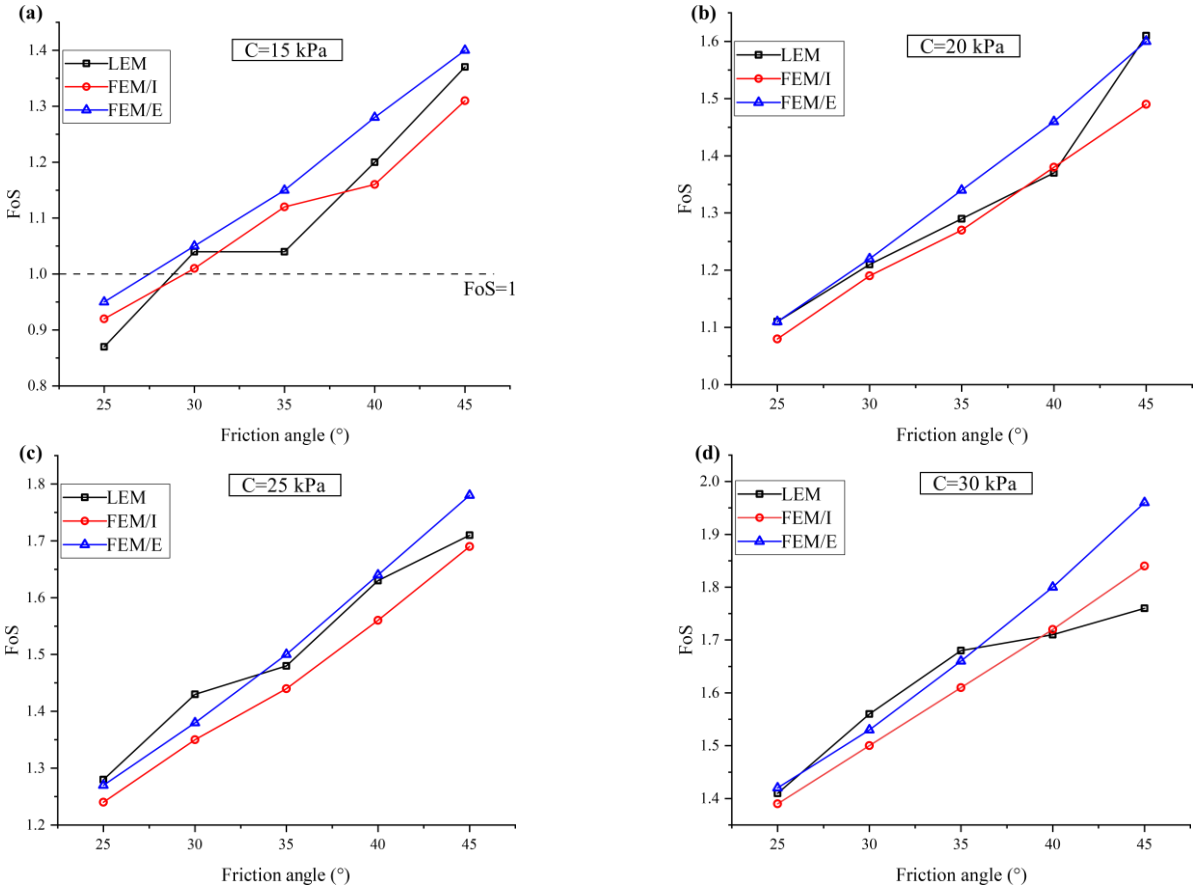

Fig. 7 Results of the LEM, FEM/I and FEM/E for 1 H-2 V slope

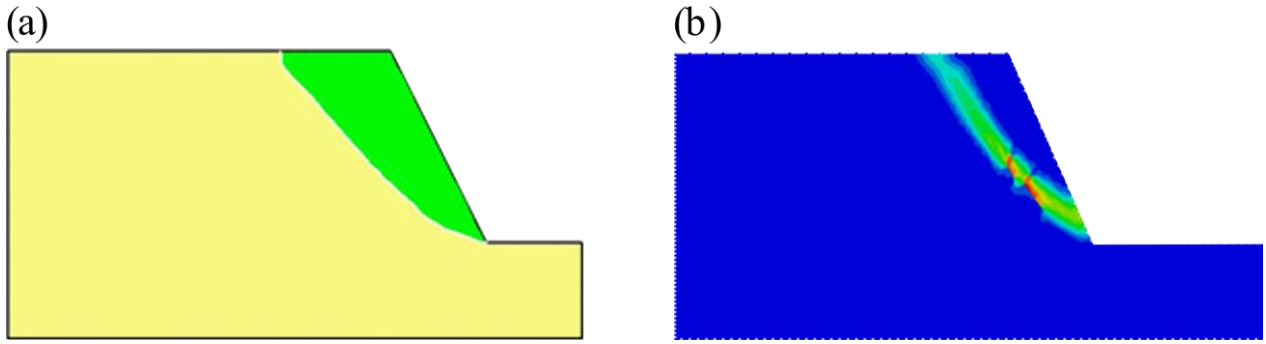

Fig. 8 Shape of the critical slip surface for soil with φ=40º, C=25 kPa (a) LEM (FoS=1.63) and (b)FEM/E (FoS=1.64)

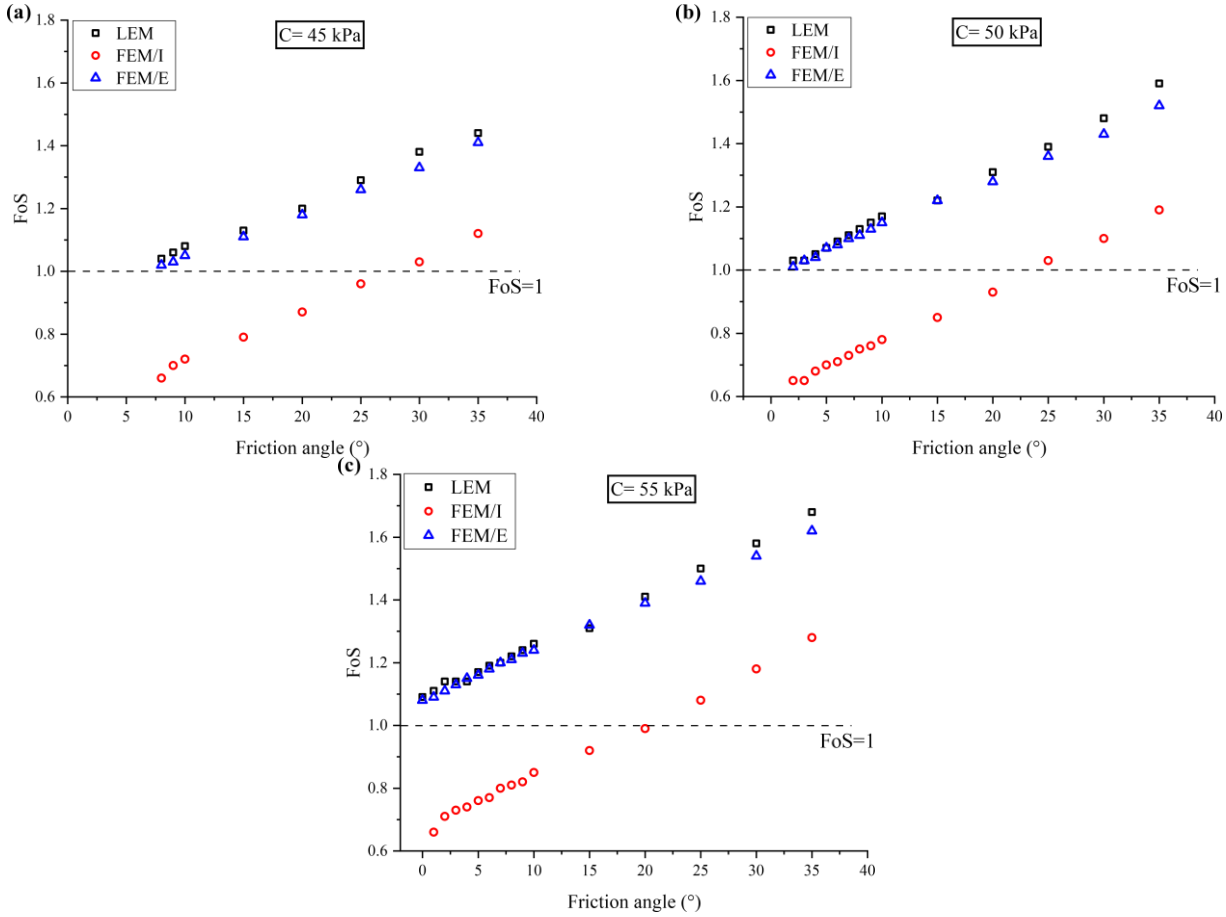

Fig. 9 Results of the FEM/E, LEM, and FEM/I for a vertical cut

changes in the magnitude of the strength parameters.

Fig. 6 presents the shear strain contour related to the minimum FoS for the FEM/E and the critical slip surface based on the LEM analysis. From this figure, there is good agreement between the shape and depth of the critical slip surface based on the proposed method and the LEM.

3.3 Slope 1 H-2 V

Fig. 7 compares the minimum FoS for the 1 H-2 V slope based on the proposed method, LEM and FEM/I. The friction angle (φ) changed from 25º to 45º in five-degree intervals, and the cohesion was selected as 15, 20, 25, and 30 kPa. According to Fig. 7, the results of the proposed method show a smooth increase in the minimum FoS without any fluctuation. Fig. 7 illustrates that the minimum FoS based on the FEM/I is usually smaller than the minimum FoSs of the two other methods and the difference between FoS values for FEM/E and FEM/I generally increase with friction angle. Fig. 8 presents the contour of the shear strain related to the minimum FoS from the FEM/E and the critical slip surface based on the LEM analysis for soil with C=25 kPa and φ=40º. This figure shows that the shape of the critical slip surface in the FEM/E is similar to the critical slip surface in the LEM.

3.4 Vertical cut (Excavation)

Fig. 9 demonstrates the minimum FoS for a vertical cut based on the proposed method and its comparison with the

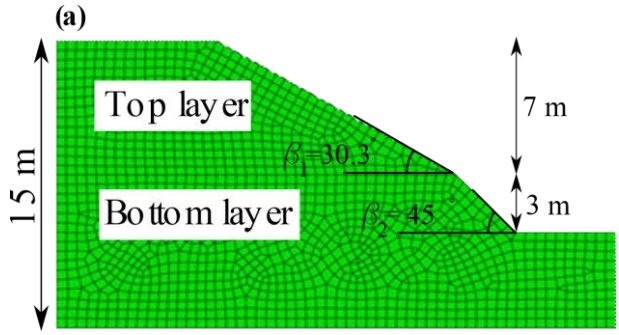

Geometry of complex model

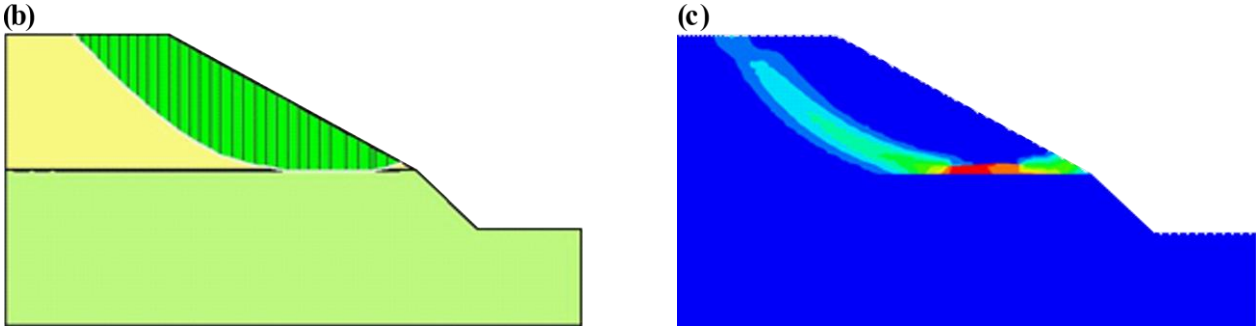

Shape of the critical slip surface for the upper layer with φ=4º, C=15 kPa and the lower layer with φ=35º, C=11 kPa (b) LEM (FoS=1.03) and (c) FEM/E (FoS=1.07)

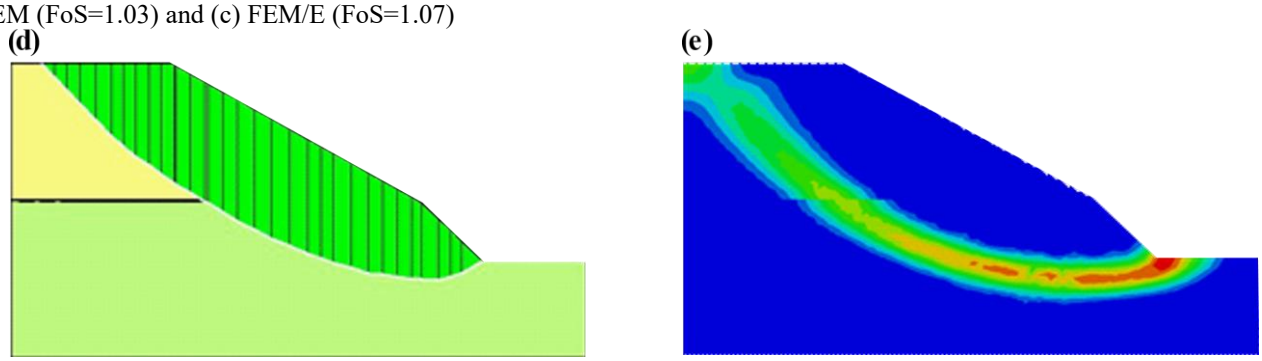

Shape of the critical slip surface for the upper layer with φ=2º, C=18 kPa and the lower layer with φ=5º, C=30 kPa (d) LEM (FoS=1.07) and (e) FEM/E (FoS=1.11)

Fig. 10 Various types of critical slip surfaces in a complex geometry

results of the LEM and FEM/I. For this geometry, the results show good agreement between the proposed method and the LEM, while a drastic drop is observed in the results of the FEM/I with respect to the two other methods. In other words, Fig. 9 suggests that it might not be economically efficient to rely on the FEM/I results for a vertical cut. To demonstrate the potential of the FEM/E for calculating the minimum FoS of a vertical cut as an extreme condition, the cohesion of the soil was changed from 45 to 55 kPa in 5 kPa intervals in Figs. 9(a) to 9(c).

The results in Fig. 9 show that iterative or implicit finite element fails to predict true FoS for steep slopes or (near) vertical slopes. From Fig. 9 and Fig. 11, one could deduce that by increasing the slope angle, the difference between FEM/I and LEM increases. Nie *et al.* (2019) stated that the criterion for slope failure associated with SRM is controversial, and divergence exists while approaching to the limit equilibrium state of slopes. Fig. 9 demonstrates although the most commonly used failure criterion is non-convergence of the solution that says when a slope arrives at the limit equilibrium state, non-convergence would occur in FEM/I, Crisfield (1997) argued the criterion is not objective enough because non-convergence does not necessarily mean the collapse of a continuum domain.

With regards to potential of the proposed method, all examples of Tu *et al.* (2016a), Dyson and Tolooiyan (2018), Griffiths and Fenton (2004), Zhu *et al.* (2015) relate to slope angle less than 53° with FoS bigger than 1. In this section, slopes with angle 30° to 90° (vertical cut) and compared to their FoS with LEM (Morgenstern and Price1965) with good agreement. This especially provides us a powerful tool to numerically analyse problems such as excavations.

3.5 Complex geometry

It is common in geotechnical research and engineering to consider multi-layer soil profiles and complex geometries (Babanouri and Sarfarazi 2018, Hou *et al.* 2019). Cala and Flisiak (2001) showed that for a two-layer embankment, the

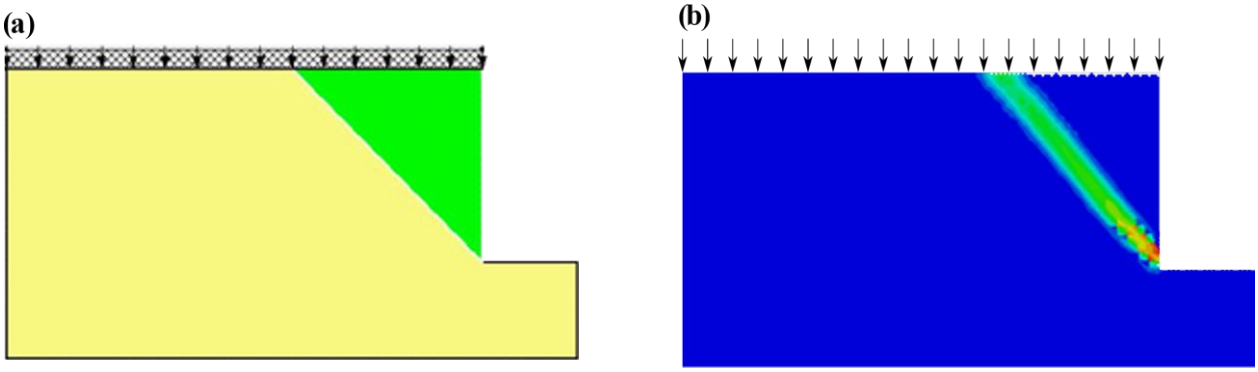

Fig. 12 Critical slip surface of a vertical cut with surcharge (q=60 kN/m^2) for soil with φ=20º, C=55 kPa (a) LEM (FoS=1.00) and (b) FEM/E (FoS=0.98)

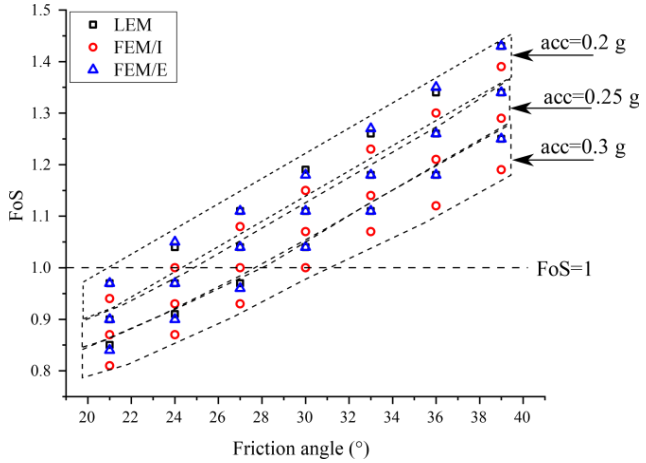

Fig. 13 Results of the FEM/E, LEM, and FEM/I for 1 H-1 V slope with pseudo-static horizontal acceleration of 0.2 g, 0.25 g and 0.3 g

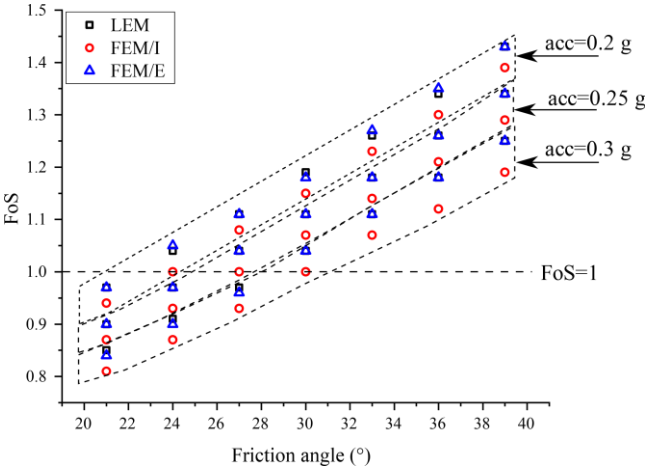

Fig. 14 Results of the FEM/E, LEM, and FEM/I for 1 H-1 V slope with pseudo-static horizontal acceleration of 0.2 g, 0.25 g and 0.3 g

magnitude of FoS obtained from LEMs are varying from the results of FLAC (Itasca 2000).

To investigate a complex condition, a slope with two layers and different slope angles for each layer (Cheng *et al.* 2007,) was considered, and Fig. 10(a) shows the geometry of the model. Sometimes in multi-layer geometries, the instability in a slope may occur in the upper layer, and the lower layer remains stable. Therefore, it is necessary to investigate the ability of the proposed method for capturing a slip surface in the upper layer and also if the slip surface passes through all the layers. Figs. 10(b) and 10(c) present a comparison between the slip surface based on the LEM and FEM/E for a condition in which the minimum FoS belongs to the critical slip surface in the upper layer. These figures show that the proposed method can capture the slip surface in the upper layer and that the shape of the critical slip

Table 1 Results of the FEM/E, LEM, and FEM/I for a complex geometry (Fig. 10(a)) with various material strength parameters for both layers

No.	Layer	Material parameters		LEM	FEM/I	FEM/E	No.	Layer	Material parameters		LEM	FEM/I	FEM/E
1	Top	c	15	1.07	1.05	1.07	9	Top	c	5	1.22	1.06	1.22
		φ	4						φ	30			
	Bottom	c	11					Bottom	c	1			
		φ	35						φ	35			
2	Top	c	20	1.37	1.34	1.36	10	Top	c	10	1.56	1.58	1.55
		φ	4						φ	30			
	Bottom	c	16					Bottom	c	6			
		φ	35						φ	35			
3	Top	c	25	1.66	1.62	1.65	11	Top	c	15	1.83	1.83	1.82
		φ	4						φ	30			
	Bottom	c	21					Bottom	c	11			
		φ	35						φ	35			
4	Top	c	20	1.61	1.59	1.6	12	Top	c	10	1.78	1.8	1.76
		φ	9						φ	35			
	Bottom	c	16					Bottom	c	6			
		φ	40						φ	40			
5	Top	c	10	1.08	1.08	1.07	13	Top	c	18	1.11	1.1	1.11
		φ	16						φ	2			
	Bottom	c	5					Bottom	c	30			
		φ	25						φ	5			
6	Top	c	15	1.33	1.32	1.32	14	Top	c	23	1.29	1.26	1.28
		φ	16						φ	2			
	Bottom	c	10					Bottom	c	35			
		φ	25						φ	5			
7	Top	c	20	1.56	1.54	1.54	15	Top	c	28	1.45	1.43	1.45
		φ	16						φ	2			
	Bottom	c	15					Bottom	c	40			
		φ	25						φ	5			
8	Top	c	15	1.53	1.53	1.51	16	Top	c	23	1.03	NA	1.01
		φ	21						φ	0			
	Bottom	c	10					Bottom	c	35			
		φ	30						φ	0			

surface in both methods is similar. Additionally, there is good similarity between the computed minimum FoS and the shape of the critical slip surface of the two methods for deep-seated failure that passes through all the layers. To provide a comprehensive comparison, Table (1) shows the results of the LEM, FEM/I and FEM/E for the geometry of Fig. 10(a) with various strength parameters. The results show that the proposed method has enough capability to calculate the minimum FoS for complex geometries.

3.6 External load

Since state of principle stresses is important for geotechnical engineering practices, the potential of proposed procedure need to evaluate for conditions in which the horizontal stresses may alter. The stability of slopes due to external loads, such as foundation and vehicle loads, is very important, and there is great interest in calculating the minimum FoS based on a stress-strain relationship. Therefore, it is necessary to show the potential of the proposed method for calculating the minimum FoS of slopes with various angles and a range of external vertical loads. In addition to external vertical loads, slopes may experience horizontal external loads. The stability of a slope subjected to psudo-static seismic coefficient will also be examined. Both vertical and horizontal external loads were applied to the model to provide a comprehensive comparison between the FEM/E, LEM, and FEM/I.

3.6.1 Surcharge

To calculate the minimum FoS of slopes bearing

external vertical loads at their top surface, a range of 10 to 60 kN/m^2 pressure load perpendicular to the top surface was applied to a 1 H-1 V slope and a vertical cut. For the 1 H-1 V slope, φ is constant for all cases and equals 20º, and C was selected as 20, 30, and 40 kPa; for the vertical cut, C=55 kPa and φ=20º were selected. Fig. 11 presents the results of the LEM/E, LEM, and FEM/I.

From Fig.11, one can deduce that similar to the slope without surcharge, the differences in the results of three methods are negligible for the 1 H-1 V slope, but in the vertical cut, the FEM/I calculates the minimum FoS far lower than those of the FEM/E and LEM. Fig. 12 illustrates that the critical slip surface calculated based on the LEM and FEM/E shows good agreement for the vertical cut with surcharge.

3.6.2 Pseudo-static horizontal acceleration

In addition to vertical external loads, the ability of the FEM/E to calculate the minimum FoS due to applying pseudo-static horizontal acceleration was investigated, and Fig. 13 shows the results of the FEM/E, LEM, and FEM/I after applying 0.2 g, 0.25 g and 0.3 g to the 1 H-1 V slope. A comparison among the minimum FoSs of the FEM/E, LEM, and FEM/I for the 1 H-1 V slope after applying pseudo-static horizontal accelerations reveals that the proposed method is capable of calculating the minimum FoS for the slope when the external horizontal stress applies to the finite element model, and its result is consistent with the LEM. According to Fig. 13, the result from the FEM/I is slightly smaller than the results from the two other methods for all horizontal accelerations.

4. Discussion

Due to the dynamic nature of explicit finite element equations (Eq. 1), an abrupt increase in the magnitude of kinetic energy shows that failure in the weakest slip surface of the soil mass is initiated. Therefore, by monitoring the magnitude of the kinetic energy, the stability or instability of the soil mass could be inferred. Duncan and Wright (1980) stated that to have trustworthy comparison between different methods, the minimum FoS for a slope should be compared because they may have different critical slip surfaces. Therefore, the minimum FoS based on the FEM/E compared with that of Morgenstern-Price's method (Morgenstern and Price 1965), which satisfies all equilibrium conditions, is a good measure for the accuracy of the FEM results with the Mohr-Coulomb constitutive model. In addition to the minimum FoS, the shape and location of the critical slip surface show good consistency between the LEM and FEM/E. To provide comprehensive investigation, the minimum FoS of a commonly used iterative finite element procedure was added. While the accuracy of the results and the ability of the proposed method are presented in previous sections, some issues need to be deeply discussed to provide a clear understanding of the simulation procedures, its advantages and limitations.

4.1 Model features

To investigate the effects of mesh dimension, the average dimension of mesh (h) to the height of the model (H=10 m) changed from 0.025 to 0.2. Fig. 14 demonstrates the distribution of quadrilateral elements for the model with a very fine and very coarse mesh. Fig. 14(a) presents the effect of mesh dimension on the minimum FoS calculated based on the strength reduction method in the FEM/E and shows that increasing the dimension of the mesh results in a higher value of the FoS (approximately 8%). A similar effect was detailed using the FEM/I with a triangular mesh (Tschuchnigg *et al.* 2015). By increasing the mesh dimension, the number of Gauss points in the possible critical slip surface decreases, and as a result, the accuracy of the simulation decreases. On the other hand, decreasing the average dimension of the mesh causes the number of elements to increase and the critical time step to decrease, and both increase the execution time. Therefore, adopting an optimum mesh dimension is necessary to have sufficient accuracy for the results and to reduce the runtime. Fig. 15(a) shows that for a small to medium mesh (h/H = 0.05-0.1), the calculated minimum FoS changed slightly. This study selected $\frac{h}{H} = 0.05$ for all models in the results section, and the calculated data showed that this magnitude could provide enough accuracy.

The explicit method is conditionally stable, and it needs to apply loads incrementally. Therefore, the time increment must be effectively small to obtain accurate results. Another effect of the mesh dimension in the FEM/E is changing the critical time step of the simulation (Eq. 2). Fig. 15(b) demonstrates the effect of the critical time step on the minimum FoS of slopes. This figure shows that decreasing the magnitude of the critical time step approximately 100 times has no effect on the final result.

4.2 Constitutive model

Applying the non-associated flow rule leads to non-uniqueness of the solution (Rice 1976, Tschuchnigg *et al.* 2015 a,b) and may cause numerical instability without indication of the failure mechanism (Nordal 2008). However, Cheng *et al.* (2007) showed that for problems with friction angles up to 35º, applying the associated or non-associated flow rule has a negligible influence on the minimum FoS, and the results of both approaches are close. In the current study, we applied the associated flow rule for the Mohr-Coulomb constitutive model for soil with friction angles up to 45º (Figs. 3, 5 and 11), and the results showed excellent consistency between the LEM and FEM/E for both the minimum FoS and the shape of the critical slip surface.

The effect of pore pressure values was neglected in this study because ABAQUS/Explicit could not execute multi-phase medium. However, this is not a large concern, as Duncan (1996) stated that the magnitude of the pore pressure is usually estimated at the time of slope failure and its accuracy is under question. Therefore, for saturated conditions, applying water pressure similar to the external load on slope surface(s) (see Griffiths and Lane1999) and using total unit weight could rectify this discrepancy.

For undrained conditions (φ=0º) in homogenous soil, the shape of the failure surface depends on the angle of the

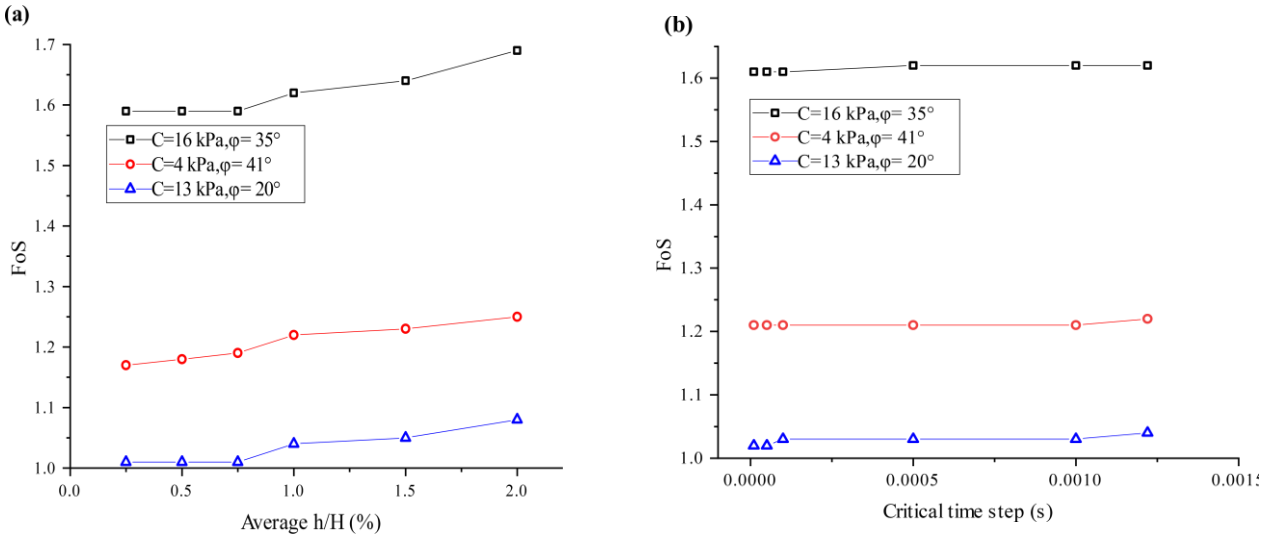

Fig. 15 Dependency of results (a) to mesh dimension and (b) to critical time step

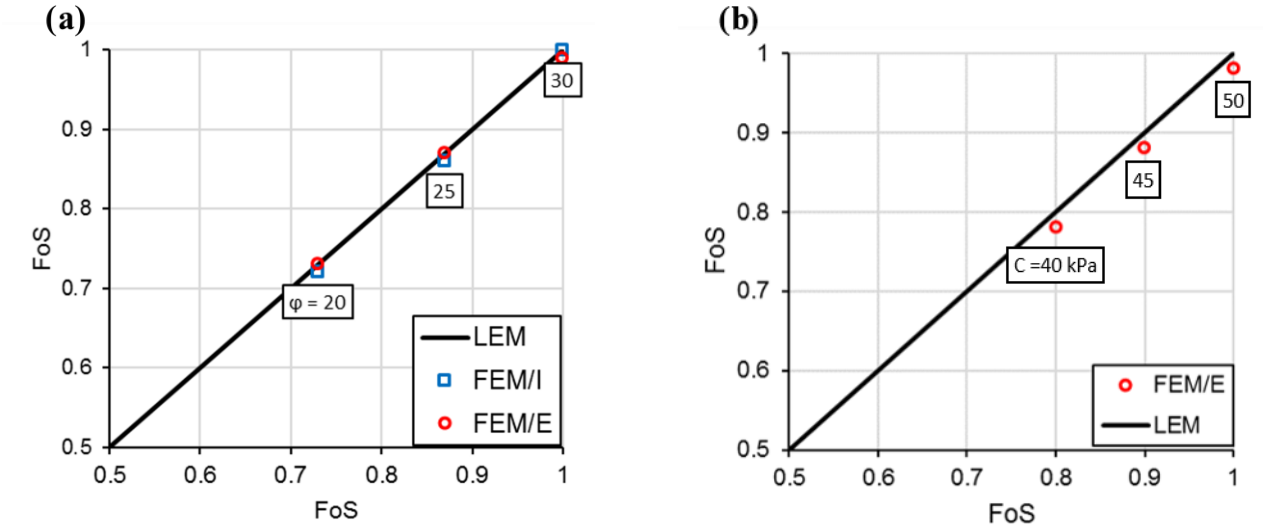

Fig. 16 Results for FoS<1 (a) 1 H-1 V slopes with C=6 kPa and (b) vertical cut with φ=0º

slope and varies from deep failure for slopes with angles less than 53º to shallow failure surfaces for slopes with higher angles (Zhu *et al.* 2015). The potential of the proposed procedure to capture deep failure is demonstrated in Fig. 8. In complex conditions, deep failure may occur only for the upper layer or the lower layer, depending on the strength parameters of the layers.

In the LEM methods, researchers assume that the behaviour of soil is ductile and that the method could not provide information about the magnitude or variation in the strains within the soil. Therefore, the mobilised shear strength may have different values along the slip surface (Duncan 1996). On the other hand, the FEM/I performs based on a constitutive model, but it needs to iterate based on a predefined iteration number according to user judgement. Therefore, due to excessive/insufficient iterations, the final displacement and shear strain are unreliable. The proposed methodology provides realistic information about the stress-strain condition of the critical slip surface at the beginning of failure.

4.3 Initial instability

Geotechnical researchers and engineers may face weak soils or inadequate data for evaluating the slope stability condition and should make judgements based on their knowledge or applying the random finite element method (RFEM), which could cause initial instability in the slope (Griffiths *et al.* 2004), and it is inevitable to encounter initial instability in their analyses.

Fig. 16(a) shows that for FoS<1, the results of the FEM/I and FEM/E are very close to the LEM. In Fig. 16(b), the FoS of a vertical cut with undrained soil (φ=0º) is presented. From this figure, one can deduce that the proposed criterion has enough capability to calculate the minimum FoS smaller than one for undrained conditions for vertical cuts, and the results are consistent with the LEM.

For initial instability, it should be noted that applying extremely low strength parameters may lead to excessive mesh distortion and execution abortion or an unacceptable increase in the kinetic energy to internal energy ratio, which

could result in unrealistic outcomes.

4.4 Geometry

This study investigates the applicability of the FEM/E for calculating the minimum FoS of slopes with angles from 33.7º to 90º and for multi-layer and multi-angle slopes. The results demonstrate that it has enough accuracy to predict the critical slip surface and the minimum FoS for conventional complex geometries in geotechnical engineering. However, for unusual shapes or complex geometry, local minima may affect the minimum FoS of the model. In these cases, the geometry of the model should be changed by altering the local gradient or by applying superficial higher-strength material parameters to the local unstable geometry to find a more general minimum slip surface. Similar to other proposed methods for calculating the minimum FoS, it is crucial to understand the procedure and keeping its limitations in perspective to have accurate judgements about slope stability or slope failure.

5. Conclusions

For many years, the LEM and FEM/I have been the most popular methods for calculating the minimum FoS and critical slip surface. While the absence of a stress-strain relationship for the LEM method caused inadequate information about stress and displacement distribution in the soil, the FEM/I method uses constitutive models to overcome this discrepancy. However, the results for extremely steep slopes show a gap between the LEM and FEM/I results.

• In this study, we proposed and examined a methodology based on strength reduction method and explicit finite element. The proposed a methodology is based on monitoring the kinetic energy in the soil domain. When applying the Mohr-Coulomb constitutive model, the minimum FoS can be calculated as the minimum factor required to reduce the soil strength for imminent failure.

• For slope angles 45° or less, there is good agreement among the minimum FoSs of three methods, but for steep slopes and vertical cuts (similar to the excavation condition), the conventional FEM/I could not predict the minimum FoS and its solution is unrealistic and shows significant differences with the LEM, but the proposed method shows excellent consistency with the LEM.

• Calculating the minimum FoS due to change of stress conditions was examined. The minimum FoS, for slopes with surcharges or subjected to pseudo-static earthquake loading, and the consistency between the results of the LEM and FEM/E showed that this method could be used for practical and scientific projects.

• This study investigates the applicability of the FEM/E for calculating the minimum FoS of slopes with angles from 33.7º to 90º and for multi-layer and multi-angle slopes. The results demonstrate that it has enough accuracy to predict the critical slip surface and the minimum FoS for conventional complex geometries in geotechnical engineering.

References

Abusharar, S.W. and Jie H. (2011), "Two-dimensional deep-seated slope stability analysis of embankments over stone column-improved soft clay", *Eng. Geol.*, **120**(1-4), 103-110. https://doi.org/10.1016/j.enggeo.2011.04.002.

Babanouri, N. and Sarfarazi, V. (2018), "Numerical analysis of a complex slope instability: Pseudo-wedge failure", *Geomech. Eng.*, **15**(1), 669-676. https://doi.org/10.1016/j.enggeo.2011.04.002.

Bathe, K.J. (2014), *Finite Element Procedures*, Prentice-Hall, U.S.A.

Brinkgreve, R.B.J., Kumarswamy, S. and Swolfs, W.M. (2016), *Plaxis 2014*, PLAXIS Bv, The Netherlands.

Cala, M. and Flisiak, J. (2001), *Slope Stability Analysis with FLAC and Limit Equilibrium Methods*, in *FLAC and Numerical Modeling in Geomechanics*, CRC Press.

Cheng, Y.M., Lansivaara, T. and Wei, W.B. (2007), "Two-dimensional slope stability analysis by limit equilibrium and strength reduction methods", *Comput. Geotech.*, **34**(3), 137-150. https://doi.org/10.1016/j.compgeo.2006.10.011.

Crisfield, M.A. (1997), *Non-linear Finite Element Analysis of Solids and Structures: Advanced Topics*, *Vol. 2*, John Wiley & Sons.

Dawson, E.M., Roth, W.H. and Drescher, A. (1999), "Slope stability analysis by strength reduction", *Geotechnique*, **49**(6), 835-840. https://doi.org/10.1680/geot.1999.49.6.835.

Dawson, E., Motamed, F., Nesarajah, S. and Roth, W. (2000), *Geotechnical Stability Analysis by Strength Reduction*, in *Slope Stability*, 99-113.

Duncan, J.M. and Wright, S. (1980), "The accuracy of equilibrium methods of slope stability analysis", *Eng. Geol.*, **16** (1-2), 5-17. https://doi.org/10.1016/0013-7952(80)90003-4.

Duncan, J.M. (1996), "State of the Art: Limit equilibrium and finite-element analysis of slopes", *J. Geotech. Eng.*, **122**(7), 577-596. https://doi.org/10.1061/(ASCE)0733-9410(1996)122:7(577).

Dyson, A.P. and Tolooiyan, A. (2018), "Optimisation of strength reduction finite element method codes for slope stability analysis", *Innov. Infrastruct. Solutions*, **3**(1), 38. https://doi.org/10.1007/s41062-018-0148-1.

Dyson, A.P. and Tolooiyan, A. (2019), "Prediction and classification for finite element slope stability analysis by random field comparison", *Comput. Geotech.*, **109**, 117-129. https://doi.org/10.1016/j.compgeo.2019.01.026.

Griffiths, D.V. and Fenton, G.A. (2004), "Probabilistic slope stability analysis by finite elements", *J. Geotech. Geoenviron. Eng.*, **130(**5), 507-518. https://doi.org/10.1061/(ASCE)1090-0241(2004)130:5(507).

Griffiths, D.V. and Lane, P.A. (1999), "Slope stability analysis by finite elements", *Geotechnique*, **49**(3), 387-403. https://doi.org/10.1680/geot.1999.49.3.387.

Griffiths, D.V. and Marquez, R.M. (2007), "Three-dimensional slope stability analysis by elasto-plastic finite elements", *Geotechnique*, **57**(6), 537-546. https://doi.org/10.1680/geot.2007.57.6.537.

Hou, C., Zhang, T., Sun, Z., Dias, D. and Li, J. (2019), "Discretization technique for stability analysis of complex slopes", *Geomech. Eng.*, **17**(3), 227-236. https://doi.org/10.12989/gae.2019.17.3.227.

Itasca, FLAC. (2000), *Fast Lagrangian Analysis of Continua*, Itasca Consulting Group Inc., Minneapolis, Minnesota, U.S.A.

Kaveh, A., Hamze-Ziabari, S.M. and Bakhshpoori, T. (2018), "Soft computing-based slope stability assessment: A comparative study", *Geomech. Eng.*, **14**(3), 257-269. https://doi.org/10.12989/gae.2018.14.3.257.

Krahn, J. (2004), *Stability Modeling with SLOPE/W*, in *An*

Engineering Methodology: First Edition, Revision 1, 396.

Li, X. W., Yuan, X. and Li, X.W. (2012), *Analysis of Slope Instability Based on Strength Reduction Method*, in *Applied Mechanics and Materials*, Trans Tech Publications.

Liu, L.L., Cheng, Y.M. and Zhang, S.H. (2017), "Conditional random field reliability analysis of a cohesion-frictional slope", *Comput. Geotech*., **82**, 173-186. https://doi.org/10.1016/j.compgeo.2016.10.014.

Liu, Y., Zhang, W., Zhang, L., Zhu, Z., Hu, J. and Wei, H. (2018), "Probabilistic stability analyses of undrained slopes by 3D random fields and finite element methods", *Geosci. Front*., **9**(6), 1657-1664. https://doi.org/10.1016/j.gsf.2017.09.003.

Manzari, M.T. and Mohamed A.N. (2000), "Significance of soil dilatancy in slope stability analysis", *J. Geotech. Geoenviron. Eng*., **126**(1), 75-80. https://doi.org/10.1061/(ASCE)1090-0241(2000)126:1(75).

Matsui, T. and Ka-Ching S. (1992), "Finite element slope stability analysis by shear strength reduction technique", *Soils Found*., **32**(1), 59-70. https://doi.org/10.3208/sandf1972.32.59.

Morgenstern, N R u, and V Eo Price. (1965), "The analysis of the stability of general slip surfaces", *Geotechnique*, **15**(1), 79-93. https://doi.org/10.1680/geot.1965.15.1.79

Naeij, M., Soroush, A. and Javanmardi, Y. (2019), "Numerical Investigation of the Effects of Embedment on the Reverse Fault-Foundation Interaction", *Comput. Geotech*., **113**, 103098. https://doi.org/10.1016/j.compgeo.2019.103098.

Naeij, M. and Soroush, A. (2021), "Comprehensive 3D numerical study on interaction between structure and dip-slip faulting", *Soil Dyn. Earthq. Eng*., **140**, p.106285. https://doi.org/10.1016/j.soildyn.2020.106285.

Nie, Z., Zhang, Z. and Zheng, H. (2019), "Slope stability analysis using convergent strength reduction method", *Eng. Anal. Boundary Elements*, **108**, 402-410. https://doi.org/10.1016/j.enganabound.2019.09.003.

Nordal, S. (2008), "Can we trust numerical collapse load simulations using nonassociated flow rules", *Proceedings of the 12th International Association for Computer Methods and Advances in Geomechanics*, Goa, India, October.

Rice, J.R. (1976), "Theoretical and applied mechanics", *Proceedings of the 14th IUTAM Congress,* North-Holland, Amsterdam, Netherlands.

Simulia, Dassault Systèmes. (2014), *Abaqus 6.14 Analysis User's Guide*.

Tschuchnigg, F., Schweiger, H.F. and Sloan, S W. (2015), "Slope stability analysis by means of finite element limit analysis and finite element strength reduction techniques. Part I: Numerical studies considering non-associated plasticity", *Comput. Geotech*., **70**, 169-177. https://doi.org/10.1016/j.compgeo.2015.06.018.

Tschuchnigg, F., Schweiger, H.F. and Sloan, S.W. (2015), „Slope stability analysis by means of finite element limit analysis and finite element strength reduction techniques. Part II: Back analyses of a case history", *Comput. Geotech*., **70**, 178-189. https://doi.org/10.1016/j.compgeo.2015.07.019

Tu, Y., Zhong, Z., Luo, W., Liu, X. and Wang, S. (2016a), "A modified shear strength reduction finite element method for soil slope under wetting-drying cycles", *Geomech. Eng*., **11**(6), 739-756. https://doi.org/10.12989/gae.2016.11.6.739.

Tu, Y., Liu, X., Zhong, Z. and Li, Y. (2016b), "New criteria for defining slope failure using the strength reduction method", *Eng. Geol*., **212**, 63-71. https://doi.org/10.1016/j.enggeo.2016.08.002.

Xu, B, and Low, B.K. (2006), "Probabilistic stability analyses of embankments based on finite-element method", *J. Geotech. Geoenviron. Eng.,* **132**(11), 1444-1454. https://doi.org/10.1061/(ASCE)1090-0241(2006)132:11(1444).

Wei, Y., Zonghong, L., Jiandong, N., Wei, W., Jiaxin, L. and Weidong, S. (2020), "Rapid calculation method for the factor of safety of a uniform slope", *Int. J. Geomech*., **20**(7), 06020012. https://doi.org/10.1061/(ASCE)GM.1943-5622.0001712.

Zhao, L., Xia, P., Xie, R., Li, L., Zhang, Y. and Cheng, X. (2017), "Stability analysis of homogeneous slopes with benches", *Geomech. Eng*., **13**(3), 517-533. https://doi.org/10.12989/gae.2017.13.3.517.

Zhu, H., Griffiths, D.V., Fenton, G.A. and Zhang, L.M. (2015). "Undrained failure mechanisms of slopes in random soil", *Eng. Geol*., **191**, 31-35. https://doi.org/10.1016/j.enggeo.2015.03.009.

Zienkiewicz, O.C., Humpheson, C. and Lewis, R.W. (1975), "Associated and non-associated visco-plasticity and plasticity in soil mechanics", *Geotechnique*, **25**(4), 671-689. https://doi.org/10.1680/geot.1975.25.4.671.

IC